ISSN 1062-7391, Journal of Mining Science, 2013, Vol. 49, No. 3, pp. 413–425. © Pleiades Publishing, Ltd., 2013.
Original Russian Text © N.I. Aleksandrova, 2013, published in Fiziko-Tekhnicheskie Problemy Razrabotki Poleznykh Iskopaemykh, 2013, No. 3, pp. 91–106.

ROCK FAILURE

Numerical-Analytical Investigation into Impact Pipe Driving in Soil with Dry Friction. Part II: Deformable External Medium

N. I. Aleksandrova

N.A. Chinakal Institute of Mining, Siberian Branch, Russian Academy of Sciences,
Krasnyi pr. 54, Novosibirsk, 630091 Russia
e-mail: alex@math.nsc.ru

Received March 16, 2013

Abstract—Under analysis is propagation of P-waves in an elastic pipe partly embedded in soil with dry friction. The mathematical formulation of the problem on impact pipe driving in soil is based on the model of axial vibration of an elastic bar, considering lateral resistance described using the law of solid dry friction. The author solves problems on axial load on pipe in interaction with external elastic medium, and compares the analytical and numerical results obtained with and without accounting for the external medium deformability.

Keywords: Axial waves, elastic bar, dry friction, pulsed loading, numerical modeling

The problems on the behavior of pipes in soil appear in many engineering procedures such as driving and pulling of piles, trenchless laying of underground utilities, underground pipework laying. Motion of various rods in mechanical systems always goes with friction. It is important to understand the influence exerted on wave process by friction of external environment and side surface of a pipe or a rod. Research of the interaction of bodies with friction is extensive [1–40].

The wave processes in rods embedded in a medium were first considered by Gersevanov [11] in 1930, based on Saint-Venant's theory. Later on, propagation of P-waves in a rod with constant-amplitude and different-oriented dry friction was an object of study [7–25]. These studies assumed the rod was driven in the nondeformable medium. A general approach to solving such problems is reducing the nonlinear problem to a set of successively solved linear problems. It is required to define boundaries in time and axial coordinate for domains where friction has constant value and orientation. The axis of friction depends on the sign of the wave velocity. Solution in each of the domains is constructed considering the preliminary determined sign of the velocity. This approach allowed solving a lot of problems with sufficiently simple laws of loading exerted on the rod.

The nonstationary and stationary one-dimensional problems on pipe and soil interaction by the law of external dry friction in the framework of the model of sonic and ultrasonic flow of a finite and infinite rod can be found in [8, 13, 15], and the two-dimensional problem of pipe driving in soil is discussed in [19].

Many researchers focused on problems on piling [26–35]. In [26] experimental data on hammer accelerations are used to calculate distribution of soil resistance along a pile. In [27] a simple dynamic model is offered to find soil resistance coefficient in the course of piling; the calculated results are compared with the dynamic testing database, and it is discussed how to use the soil resistance model in the wave equation of the pile motion. Dynamic analysis of side surface of pile uses boundary element approach in [28], and the finite element method is chosen to solve axially symmetric two-dimensional problem on piling, with algorithm of slip friction contact on the pile and soil interface in [29, 30]. Experiments on influence exerted by soil plug inside an open-end driven pile on the static and dynamic response of the pile are described in [31]. In [32], based on analysis of the wave

equation from [22], the load-bearing capacity of piles is calculated and compared with the experimental results. The problem on piling in [33, 34] is solved with modeling the friction contact between the pile and soil using the plastic strengthening/weakening theory. The finite element analysis in [35] uses the Coulomb law of the soil and pile contact friction, and the estimates are compared with the experimental data. Many experimental approaches to pipe driving in soil are reviewed in [36–40]. However, the researchers [26–40] left the nonstationary problems on the pile and soil interaction aside of their attention.

The dynamic problem on wave propagation in a composite material composed of fiber and binder with dry friction value pre-set at their interface is discussed in [41]. Motion of the fiber and binder is described with one-dimensional wave equations solved analytically and using the finite element method. The load was assumed linearly growing in time. The main attention was paid to the perturbance delay as against the wave propagation.

The given study continues the research presented in [21], considering deformation of the surrounding medium, compares the results of the both models and identifies the applicability of the simple model. The author uses the end-to-end numerical calculation of wave processes as systems with dry friction, that allows analyzing any type loading. The obtained approximate analytical solutions of the one-dimensional problem on radially oriented perturbance propagation during the slip-free elastic medium and pipe interaction and axial load applied to the pipe end are the test patterns for the finite difference solutions of two-dimensional problems with the pre-set elastic interaction or dry friction on the pipe and medium contact.

1. PROBLEM FORMULATION

The mathematical formulation of the problem on pipe driving in soil is based on the model of longitudinal oscillations of elastic rod, considering lateral resistance. We solve the mixed dynamic axially symmetric problem on interaction of an elastic cylinder pipe and an elastic soil layer. The pipe end is applied with a longitudinal impact. The pipe motion is described with a one-dimensional wave equation, lateral resistance of soil (infinitesimal strains)—using simplified models of elastic medium, and yielding—by the dry friction law.

An elastic tubular rod (*R*—radius; *h*—wall thickness) with length *L* is embedded in soil for the length L_1. The applied longitudinal half-sine impact impulse has amplitude Q_0 and duration t_0:

$$Q(t) = Q_0 \sin(\omega_* t) H(t_0 - t) H(t), \quad \omega_* = \pi / t_0, \tag{1}$$

where H is Heaviside's step function.

Let the origin of the coordinate system be the impacted end of the rod, and the *z* axis be oriented in parallel to the driven rod axis. The rod motion is described with the one-dimensional wave equation in terms of displacements $U(t,z)$:

$$\ddot{U} = c^2 U''_{,zz} + \tau(z, \varepsilon_{rz}). \tag{2}$$

Here, $c = \sqrt{E/\rho}$ is wave velocity in the rod; *E* is Young's modulus; ρ is the rod material density; τ is response of the medium.

Initial conditions are zero:

$$U\big|_{t=0} = 0, \quad \dot{U}\big|_{t=0} = 0. \tag{3}$$

At the rod end $z = 0$ the stress is assigned, the rod end $z = L$ is stress-free:

$$ESU_{,z}\big|_{z=0} = -Q(t), \quad ESU_{,z}\big|_{z=L} = 0, \tag{4}$$

where $S = \pi h(2R - h)$ is the tubular rod cross-section area.

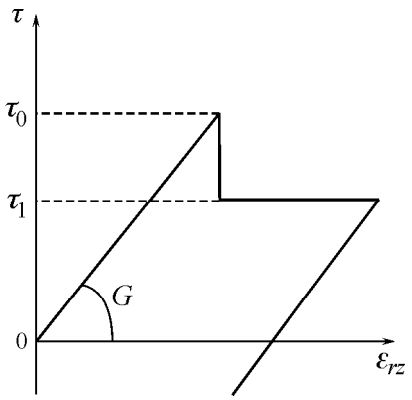

Fig. 1. Relation of response of the medium and shear strain ε_{rz} .

The curve $\tau(\varepsilon_{rz})$ fits in the elastoplastic deformation diagram, taking account of yielding peak (Fig. 1). The diagram contains an elastic line from 0 to τ_0 showing the rod and medium adhesion, then ultimate shear stress τ_0 changes to τ_1 and frictional slip starts (usually proportional to pressing force). When the current rod cross-section $z > L - L_1$ stops, the rod and medium adhere again, and the adherence can later be broken by stress waves arrived from the rod ends. Orientation of friction forces is governed by the sign of velocity of these waves. The present study assumes $\tau_0 = \tau_1$.

At the elastic stage when $|\tau| < \tau_0$, the shear stress of soil is found using a two-dimensional model of the medium with single displacement V in the line of z:

$$\ddot{V} = a^2 V_{,zz} + b^2 \left(V_{,rr} + \frac{1}{r} V_{,r} \right), \quad a^2 = \frac{\lambda + 2G}{\gamma}, \quad b^2 = \frac{G}{\gamma}. \tag{5}$$

Here, G is shear modulus; λ is Lamé's coefficient; γ is soil density; r is radial coordinate. Equation (5) is the model of the medium, including compressibility of soil along the rod axis (coefficient a^2), shearing resistance (coefficient b^2) and inertance of soil particles moving along the rod axis.

This model was used to solve many dynamic and static problems in [42], and it was shown that amplitudes of axial strains and their partial derivatives are much higher than these values in radial direction. This allows transfer from the accurate model of the elastic theory to the physically equal and mathematically simpler model of medium deformation with the single displacement (5).

Boundary condition for (5) in the absence of friction slip on the rod surface is:

$$V(z,r)\big|_{r=R} = U(z), \quad L - L_1 \le z \le L. \tag{6}$$

It defines the equality of the displacements of the rod and soil on the rod surface. The other boundary conditions are the absence of displacements at the exterior boundary $r = R_2$ of soil and the absence of stresses on the free surfaces of soil:

$$V(z,r)\big|_{r=R_2} = 0 \quad (L - L_1 \le z \le L), \quad V_{,z}(z,r)\big|_{z=L-L_1} = 0, \quad V_{,z}(z,r)\big|_{z=L} = 0. \tag{7}$$

The soil response τ is:

$$\tau(z,t) = \frac{P}{S\rho} \begin{cases} GV_{,r}\big|_{r=R}, & z > L - L_1, \\ 0, & z \le L - L_1. \end{cases} \tag{8}$$

Here, $P = 2\pi R$ is perimeter of the tubular rod.

At the stage of slip when $|\tau| < \tau_0$, the rod and soil interaction is described by the dry friction law:

$$\tau(z,t)=\frac{P}{S\rho}\begin{cases}-k\tau_0, & z>L-L_1,\\ 0, & z\le L-L_1,\end{cases} \tag{9}$$

$$k=\operatorname{sign}[\dot U(z)-\dot V(z,R)] \quad \text{at} \quad \dot U-\dot V\ne 0\,.$$

During slip, friction forces on the rod and in the medium agree in value and differ in orientation, therefore, there are the following boundary conditions for the medium:

$$GV_{,r}\big|_{r=R}=k\tau_0. \tag{10}$$

The method of end-to-end calculation of wave processes in systems with dry friction, presented below, allows considering any type load as the friction value and orientation at any point of the rod and at any time moment is chosen based on physical considerations. Also, the author presents analytical estimates for some problems.

2. ANALYTICAL ALGORITHMS

The system of equations (1)–(10) was solved in the case of a unit impact, using the cross-type finite difference scheme and method of minimization of data scatter. Equation (5) is approximated as:

$$V_{ji}^{n+1}-2V_{ji}^{n}+V_{ji}^{n-1}=\left[a^2\Lambda_{jj}V_{ji}^{n}+b^2\left(\Lambda_{ii}V_{ji}^{n}+\frac{1}{r}\Lambda_i^0V_{ji}^{n}\right)\right]h_t^2\,, \tag{11}$$

where Λ_{jj}, Λ_{ii} are second-order central-difference operators in coordinates z, r; Λ_i^0 is central-difference operator of the first derivative with respect to r; $V_{ji}^{n}=V(h_tn,h_zj,r_i)$ are mesh values of displacements at time $t=h_tn$ at the point $z=h_zj$; $r_i=R+h_r(i-1)$, $i=1,2,\ldots$; h_t, h_z, h_r are mesh steps in coordinates t, z, r.

The approximation of (2) has the form:

$$U_j^{n+1}-2U_j^{n}+U_j^{n-1}=(c^2\Lambda_{jj}U_j^{n}+\tau_j^{n})h_t^2\,, \tag{12}$$

where $U_j^{n}=U(h_tn,h_zj)$, $\tau_j^{n}=\tau(h_tn,h_zj)$ are mesh values of displacements and shear stresses on the rod surface.

Conditions of stability of Eqs. (11) and (12) are:

$$h_t\le\left(\frac{a^2}{h_z^2}+\frac{b^2}{h_r^2}\right)^{-1/2}, \quad h_t\le\frac{h_z}{c}\,.$$

The optimized parameters of the finite difference mesh to make data scatter of (11) and (12) minimum are $h_z=ch_t$ axially and $h_r=h_tcb/\sqrt{c^2-a^2}$ radially.

Approximation of boundary conditions used right-hand side for two derivatives at the rod end $z=0$: $ES(U_1^{n}-U_0^{n})/h_z=-Q(t)$ and central-difference approximation at $z=L$. Similarly, we approximated boundary conditions for soil at the boundaries $z=L-L_1$ and $z=L$. For the boundary condition (6), three-point approximation was used [43].

The algorithm with friction is analogous to that in [19, 21]. Neither orientation nor value of friction force are known beforehand, and we calculate relative velocities of displacing points of the medium and rod for two optional signs of k ($k>0$ and $k<0$):

(a) When $k>0$, introduce a fictitious velocity $U_j^{+}-V_{j,1}^{+}$, where:

$$V_{j,1}^{+}=\frac{V_{j,1}^{n+1}-V_{j,1}^{n}+h_t^2\tau_0}{h_t}\,, \quad U_j^{+}=\frac{U_j^{n+1}-U_j^{n}+h_t^2\tau_0}{h_t}\,;$$

(b) When $k<0$, introduce a fictitious velocity $\dot U_j^{-}-\dot V_{j,1}^{-}$, where:

$$V_{j,1}^{-}=\frac{V_{j,1}^{n+1}-V_{j,1}^{n}-h_t^2\tau_0}{h_t},\quad U_j^{-}=\frac{U_j^{n+1}-U_j^{n}-h_t^2\tau_0}{h_t}.$$

The values of $V_{j,1}^{n+1}$ and U_j^{n+1} are calculated from (11) and (12) without regard to friction, and there are two possible situations:

1. If $\dot{U}_j^{+}-\dot{V}_{j,1}^{+}$ and $\dot{U}_j^{-}-\dot{V}_{j,1}^{-}$ have the same sign, the true displacements $V_{j,1}^{n+1}$, U_j^{n+1} out of $V_{j,1}^{+}$, U_j^{+} and $V_{j,1}^{-}$, U_j^{-} are selected as $V_{j,1}^{k}$, U_j^{k} such that:

$$(\dot{U}_j^{k}-\dot{V}_{j,1}^{k})=\min[\mathrm{abs}(\dot{U}_j^{-}-\dot{V}_{j,1}^{-}),\mathrm{abs}(\dot{U}_j^{+}-\dot{V}_{j,1}^{+})].$$

2. If $\dot{U}_j^{+}-\dot{V}_{j,1}^{+}$ and $\dot{U}_j^{-}-\dot{V}_{j,1}^{-}$ have different signs, or one of these velocities is zero, then, assuming friction is passive, the real relative velocity of the soil and rod equals zero. The soil and rod adhere and are moved together, thus, friction is absent, and the rod and soil interaction is elastic.

Accordingly, the problem on finding the interface of the relative motion and relative rest domains, which is the major difficulty in analytical solutions, reduces to finding points where $\dot{V}_{j,1}^{+}-\dot{U}_j^{+}$ and $\dot{V}_{j,1}^{-}-\dot{U}_j^{-}$ have different signs, or where one of them is zero.

The value and orientation of friction force are unambiguously defined in the calculation process, and, therefore, on each time level, we solve a linear problem with defined friction included as load in the right-hand side of equation.

Friction can be either passive or active. For instance, when particles of the soil and rod are moved in the same direction and $|\dot{V}|>|\dot{U}|$, friction accelerates the rod; otherwise, it decelerates the rod. With the same sign $\dot{V}$ and $\dot{U}$, it is deceleration that takes place.

3.ANALYTICAL ESTIMATES

The one-dimensional problem includes a thin soil layer (in the line of *z*) with radius R_2 and a pipe with radius *R* driven in soil. Motion of the medium is described with the one-dimensional wave equation in terms of the radial coordinate *r* driven from (5) under assumed neglectability of the derivatives with respect to the axis *z*:

$$\ddot{V}=b^2\left(V_{,rr}+\frac{1}{r}V_{,r}\right),\quad b^2=\frac{G}{\gamma}. \tag{13}$$

The boundary conditions:

$$V(r)\big|_{r=R}=U,\quad V(r)\big|_{r=R_2}=0. \tag{14}$$

The pipe motion equation is derived from (2) on the assumption that the relation of the displacement and *z* can be disregarded:

$$\ddot{U}=\frac{PG}{S\rho}V_{,r}\bigg|_{r=R}+\frac{Q(t)}{S\rho}. \tag{15}$$

The initial conditions are zero.

Take the Laplace transform of time with parameter *p*:

$$p^2V^L=b^2\left[(V_{,rr})^L+\frac{1}{r}(V_{,r})^L\right],\quad p^2V^L\big|_{r=R}=\frac{PG}{S\rho}(V_{,r})^L\bigg|_{r=R}+\frac{Q^L}{S\rho},\quad V^L\big|_{r=R_2}=0. \tag{16}$$

The first case to be analyzed is the infinite medium ($R_2\to\infty$). Let the pipe be applied with a step load $Q(t)=Q_0H(t)$. Using Laplace transform of a function re-writes (16) as:

$$U^L = \frac{Q_0 K_0(\eta)}{LS\rho p^2 (pK_0(\eta) + K_1(\eta) P\gamma b / S\rho)},$$

where K_0, K_1 are cylindrical functions of imaginary argument; $\eta = Rp/b$.

Asymptotic form of the Laplace transform of a function when $p \to 0$, which corresponds to $t \to \infty$ in the space of pro-images, is:

$$U^L = \frac{Q_0}{2\pi G p} \ln \frac{pCR}{2b}.$$

Converse of the Laplace transform [44] produces the asymptotic relation of the pipe displacement and time when $t \to \infty$ in the infinite medium:

$$U(t) = \frac{Q_0}{2\pi G} \ln \frac{2bt}{R}, \quad (t \to \infty). \tag{17}$$

Considering wave reflection from the external boundary $r = R_2$, image solution of (16) is:

$$U^L = \frac{Q_0}{S\rho p^2} \left(p + \frac{[K_0(\eta) I_0(\eta_2) - I_0(\eta) K_0(\eta_2)]}{[K_1(\eta) I_0(\eta_2) - I_1(\eta) K_0(\eta_2)]} \frac{P\gamma b}{S\rho} \right)^{-1}. \tag{18}$$

Here, I_0, I_1 are modified Bessel functions; $\eta = Rp/b$; $\eta_2 = R_2 p/b$.

If $t \to \infty$ ($p \to 0$), then it follows from (18) that the solution oscillates about relatively static equilibrium defined by the formula:

$$U_{stat} = \frac{Q_0}{2\pi G} \ln \frac{R_2}{R}. \tag{19}$$

Figure 2 shows the results of the finite difference solution of the system (13)–(15) by the solid lines, asymptotic solutions of (17) by the dashed lines and the static value of (19) by the dash-and-dotted line. The thick lines correspond to $R_2 = 20$ m, the thin lines— $R_2 = 2$ m. The finite difference mesh parameters were: $h_r = 0.01$ m, $h_t = h_r / b$. The other parameters were: $Q_0 = 88$ kN, $E = 210$ GPa, $h = 0.003$ m, $R = 0.045$ m, $\rho = 7530$ kg/m^3, $\gamma = 2000$ kg/m^3, $a = 611$ m/s, $b = 357$ m/s, used later as the reference parametric set. Hereinafter, the parameters of the surrounding medium corresponded to the averaged characteristics of loam.

As seen in Fig. 2, the asymptotic solution (17) accurately describes the finite difference solution in the range between the impact treatment start and the first reflected wave arrival from the external boundary. Reflections from the boundaries $r = R$, $r = R_2$ causes oscillations about relatively static value (19).

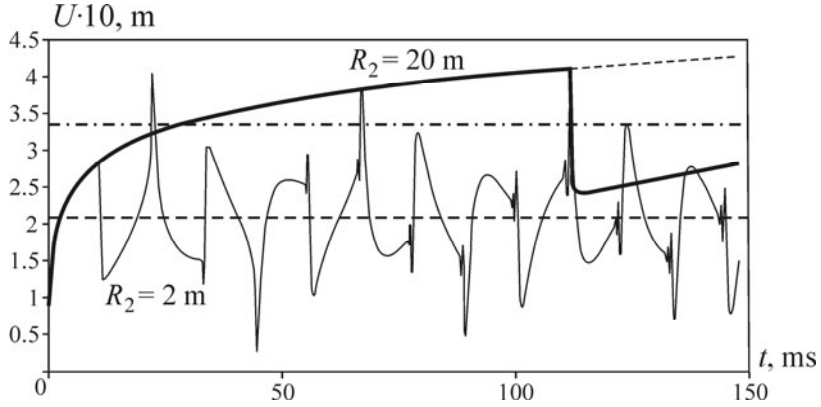

Fig. 2. Oscillograms of displacement under step loading.

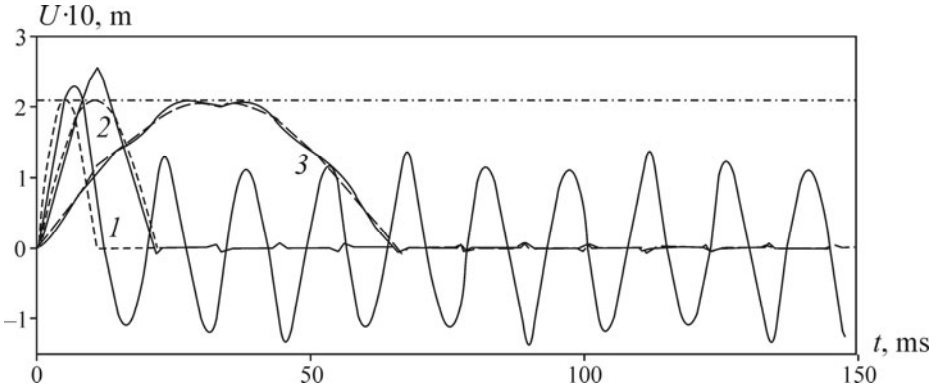

Fig. 3. Oscillograms of displacement under pulsed loading.

In case of the pulsed loading (1) of the pipe in the medium with the radius R_2, the imaged asymptotic solution of (16) has the form of:

$$U^L = \frac{Q_0\omega_*(1+e^{-p\pi/\omega_*})}{S\rho(p^2+\omega_*^2)(p^2+\beta^2)}, \quad \beta^2 = \frac{2\pi G}{S\rho\ln(R_2/R)}.$$

Converse of the above expression yields time dependence of the pipe displacements:

$$U = \frac{Q_0}{S\rho\beta(\omega_*^2-\beta^2)}\begin{cases}\omega_*\sin\beta t - \beta\sin\omega_* t, & t \le t_0,\\ \omega_*(\sin\beta t + \sin\beta(t-t_0)), & t > t_0.\end{cases}$$

If $\omega_* << \beta$, then:

$$U = U_0\begin{cases}\sin\omega_* t, & t \le t_0,\\ 0, & t > t_0.\end{cases} \qquad U_0 = \frac{Q_0}{S\rho\beta^2}. \tag{20}$$

Figure 3 illustrates calculated pulsed loading of a pipe in the medium with the fixed $R_2 = 2$ m. The pulse duration is $t_0 = 2(R_2 - R)/b$ for curve *1*, $t_0 = 4(R_2 - R)/b$ for curve *2* and $t_0 = 12(R_2 - R)/b$ for curve *3*; the other input parameters are taken from the reference parametric set. The solid lines show the finite difference solution, dashed lines—approximated solution (20); dash-and-dotted lines—U_0. The comparison of (20) and numerical results yields that if the pulse duration is divisible by time of four runs of the wave between the boundaries of the medium: $t_0 = 4n(R_2 - R)/b$ $(n = 1, 2, ...)$, then the waves reflected from the external boundary kill the pulse. As follows from Fig. 3, the pipe displacement is quantitatively and qualitatively correct described with the analytical solution (20).

4. PLANE PROBLEM ON ELASTIC INTERACTION AT THE PIPE AND SOIL INTERFACE

The finite difference calculation of the system (2)–(8) was performed for the soil layer with the thickness $L = L_1 = 0.2$ m $= 2h_z$ and radii $R_2 = 2$ m and $R_2 = 20$ m under step loading. Analysis of the solutions showed that the logarithmic dependence of the solution on time is typical of the plane problem as with the one-dimensional problem. The qualitative behavior of the both is coincident.

Figure 4 presents the numerical calculations of the pipe displacements versus time under step loading for different lengths of the pipe and thicknesses of the medium ($L = L_1$). The problem parameters were $R_2 = 20$ m, $h_z = 0.1$ m; the rest—from the reference set. The analysis showed that for the longer pipe, the value of the displacements at the cross-section $z = 0$ at $t = 100$ ms lowers in proportion to the logarithmic function: $F(L) = (898\ln L + 2061)^{-1}$, where $[F] =$ mm, $[L] =$ m. For low L (soil layer thickness in the line of z equals two steps of the mesh, $L = 2h_z$), the finite difference solution produces the higher error than $F(L)$.

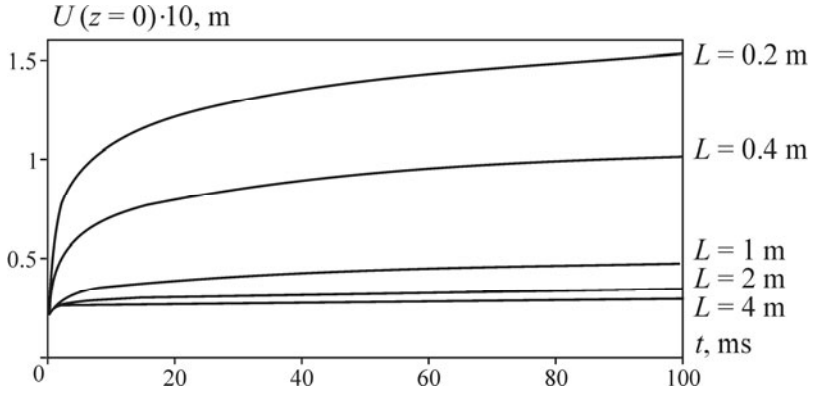

Fig. 4. Oscillograms of displacement at various lengths of the pipe under step loading.

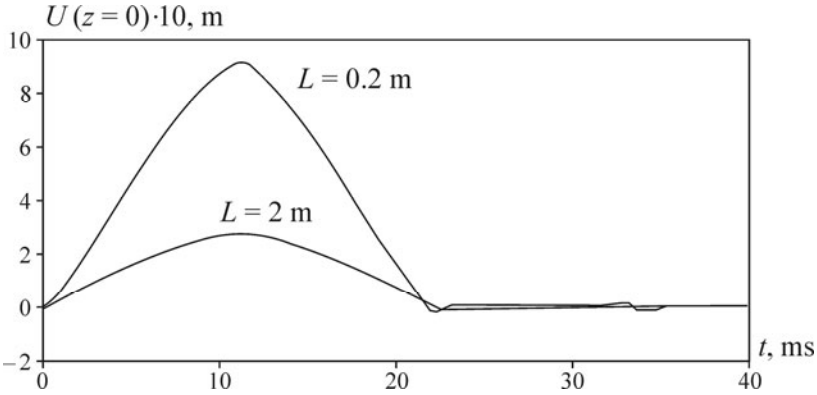

Fig. 5. Oscillograms of displacement under pulsed loading.

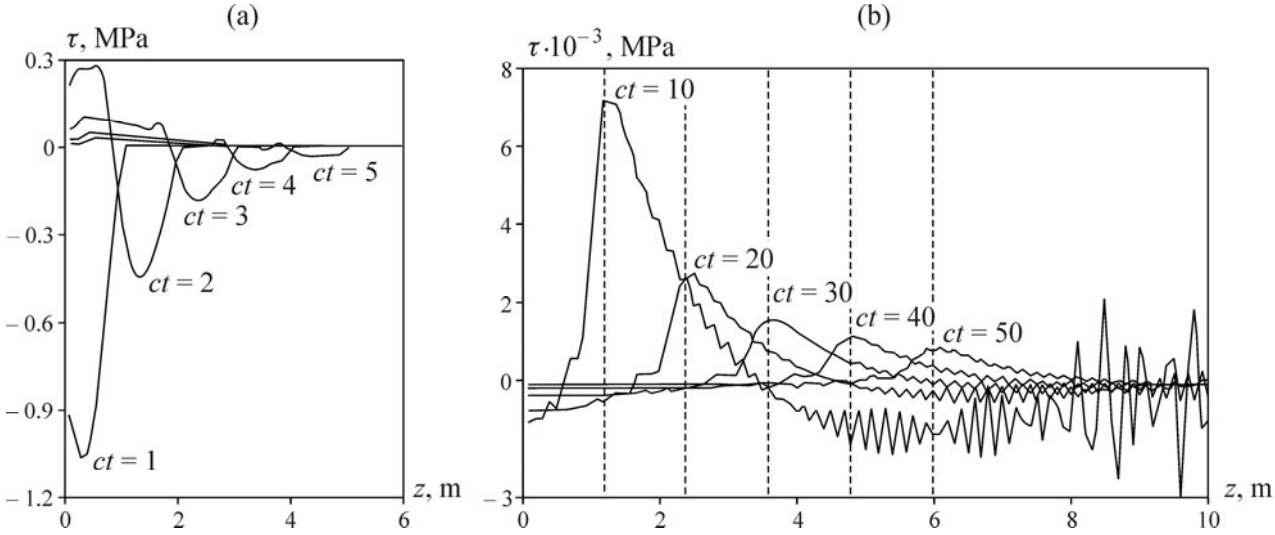

Fig. 6. Curves of shear stresses on the pipe surface at different time moments: $z = ct$, m.

The curves in Fig. 5 are shown for the pipe displacements under half-sine pulse (1) with duration $t_0 = 4(R_2 - R)/b$ at two values of L ($L = L_1$). The problem included $R_2 = 2$ m, $h_z = 0.1$ m and the other parameters from the reference set. Qualitatively, the solutions of the plane and one-dimensional problems behave the same way (compare Figs. 3 and 5).

Figure 6 shows the curves of the shear stress exerted by the soil on the pipe surface at various time moments. The input parameters were $L = 7.5$ m, $L_1 = 4$ m, $R_2 = 0.8$ m, $t_0 = 0.25$ ms and the other parameters from the reference set. The vertical dashed lines in Fig. 6b show the zone of quasi-fronts: $z = ct$.

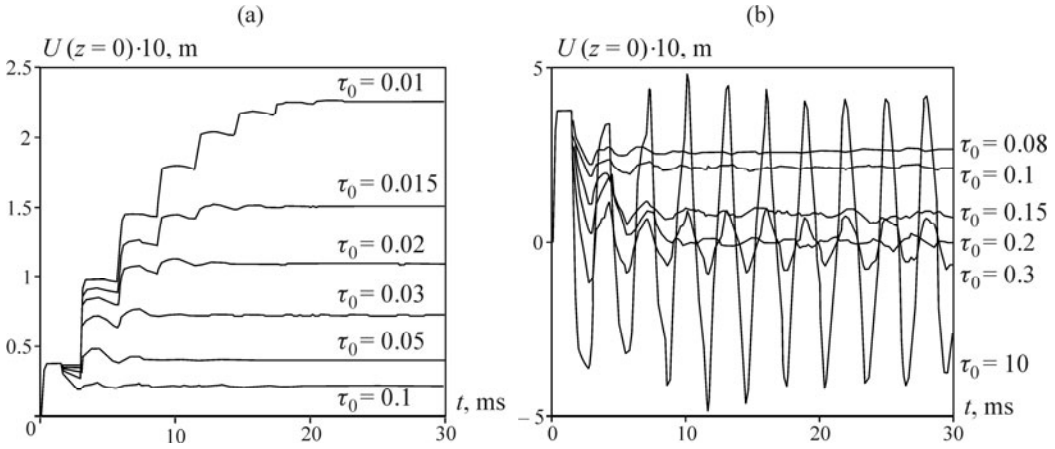

Fig. 7. Oscillograms of pipe displacement at $z = 0$: τ_0 is in MPa.

In the vicinity of the quasi-front of P-wave with velocity c in the pipe, the maximum shear stress amplitude decreases exponentially as $\sim e^{-0.85ct}$. In the vicinity of the quasi-front of P-wave in the medium, the maximum shear stress amplitude decreases as $t^{-4/3}$ (Fig. 6b). In length of time, perturbances that move with the P-wave velocity in soil start dominating. Using Fig. 6b it is possible to evaluate friction force at which the pipe starts slipping in soil, depending on the pipe length and the impact pulse amplitude.

5. PLANE PROBLEM SOLUTION CONSIDERING SLIP AT THE PIPE AND SOIL INTERFACE

Figure 7 shows the curves of displacement of the pipe end $z = 0$ versus time under half-sine impact pulse and different shear stress values: $\tau_0 = 0.1$, 0.05, 0.03, 0.02, 0.015, 0.01 MPa in Fig. 7a; $\tau_0 = 10$, 0.3, 0.2, 0.15, 0.1, 0.08 MPa in Fig. 7b. The parameters were $L = 7.5$ m, $L_1 = 4$ m, $R_2 = 0.8$ m, $t_0 = 0.22$ ms, and the rest were taken from the reference set. The value $\tau_0 = 10$ MPa conforms with the elastic interaction, the pipe end $z = 0$ oscillates around zero. The amplitude of the oscillations decreases with the decrease in the shear stress amplitude (curves $\tau_0 = 0.3$ and $\tau_0 = 0.2$ MPa in Fig. 7b) and residual displacement (curves $\tau_0 = 0.15$ and $\tau_0 = 0.1$ MPa in Fig. 7b and all curves in Fig. 7a) grows as τ_0 becomes lower. As seen in Fig. 7b, when $\tau_0 \le 2Q_0 / LP$, the pipe slips in the medium. Analysis of the displacements at $t = 100$ ms versus τ_0 showed that this dependence is close to the inverse function: $\max U(\tau_0) \approx 28\tau_0^{-1}$.

According to the calculated data on displacement of pipes of varied length, the average displacement $2U_{\text{av}} = (\max\limits_z U + \min\limits_z U)\Big|_{t=100\text{ ms}}$ is in inverse proportion to the pipe length. This result is qualitatively different from the behavior of the pipe elastically embedded in soil (see Fig. 4) for there is the logarithmic dependence in the latter case.

So, displacement of a pipe with dry friction is inverse proportional to the friction force $F_{\text{f}} = PL\tau_0$.

The calculations illustrated in Fig. 8 were performed for two models of impact pulse loading and different ultimate shear stresses. The thin curve shows model (2)–(10); the thick curve illustrates model (2)–(4), (9) disregarding external medium action from [21]. The problem parameters were $L = 7.5$ m, $L_1 = 4$ m, $R_2 = 0.8$ m, $t_0 = 0.22$ ms, and the rest were taken from the reference set. The two models reach mapping when $\tau_0 < 0.02$ MPa, i.e. when $\tau_0 < Q_0 / (4LP)$. The latter inequality means that when the pipe length is below some definite value governed by the impact pulse amplitude, the ultimate shear stress and perimeter of the pipe—$L < L_* = Q_0 / (4\tau_0 P)$—the motion of the external medium is possible to neglect and use a simpler model.

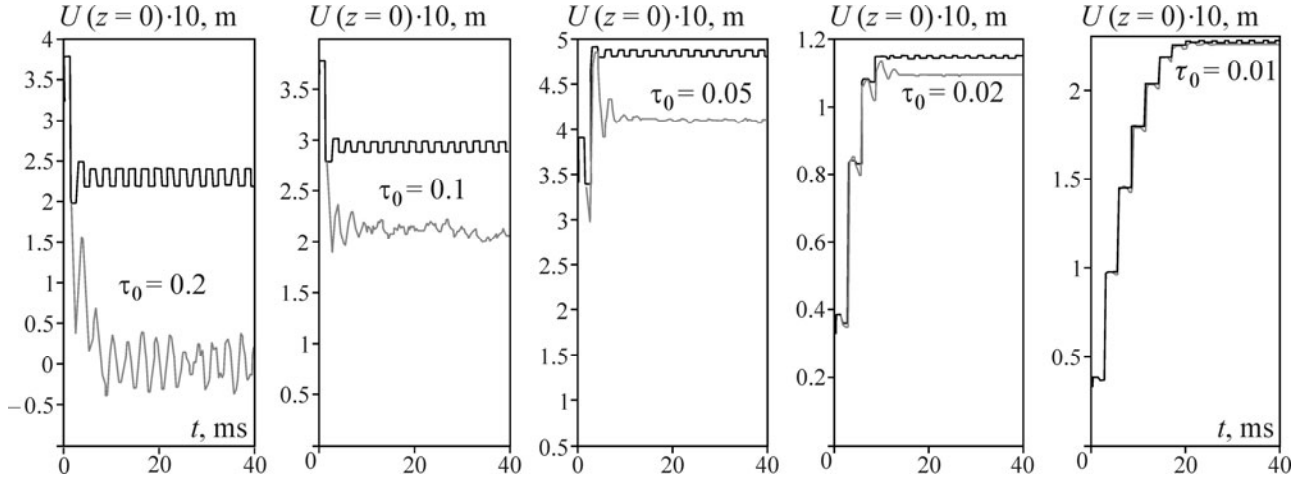

Fig. 8. Oscillograms of pipe displacement at $z = 0$: τ_0 is in MPa.

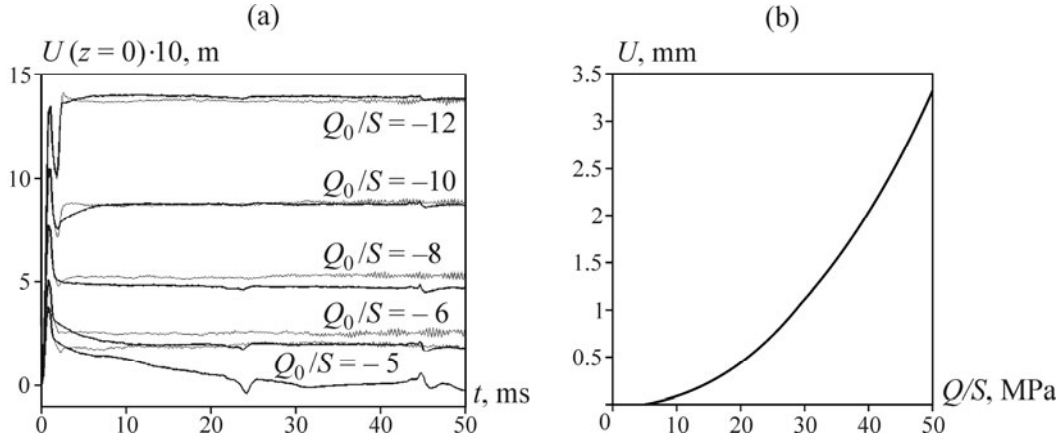

Fig. 9. (a) Oscillograms of pipe displacement at different impact pulse amplitude and (b) curve of the displacement and the impact pulse amplitude.

The oscillograms of displacement of the pipe end $z = 0$ in Fig. 9a are plotted at varied impact pulse amplitudes. The problem parameters were $L = L_1 = 4$ m, $t_0 = 1$ ms, $E = 203$ GPa, $h = 0.01$ m, $R = 0.1625$ m, $\rho = 7805$ kg/m^3, $h_z = 0.1$ m, $\tau_0 = 0.02$ MPa. The thin curves are for $R_2 = 0.2$ m and the thick curves are for $R_2 = 4$ m. Under small amplitude pulses ($Q_0 / S < 10$ MPa) or, which is of the same sort of thin, under low Q_0 / F_f, the external medium radius has influence on the residual displacement. So, when slip begins, the external medium radius has almost no effect on the wave process in the pipe. Figure 9b shows the curves of the pipe displacement at $z = 0$ at $t = 100$ ms and the impact pulse amplitude. The finite difference solution is shown by the thin curve, and its approximation described with the function $U(Q_0 / S) = 0.0014 Q_0^2 / S^2 - 0.0059 Q_0 / S - 0.008$ is displayed by the thick curve. The obtained result qualitatively confirms the deduction on that displacement is proportional to the squared amplitude of the impact pulse.

Figure 10a shows the oscillograms of displacement at different pipe lengths ($L = L_1 = 4$, 10, 20, 30 m) and different impact pulse amplitudes, $R_2 = 4$ m, the other parameters are equal to those in Fig. 9. The aim was to find the impact pulse amplitude, such that the average residual displacements are non-zero, i.e. slip start. Figure 10b shows the relationship of the impact pulse amplitude and the pipe length (solid curve) based on the analysis of the data in Fig. 10a. The approximation of this relationship is linear: $Q_0 / S \approx 0.729 L + 1.86$ (dashed curve in Fig. 10b).

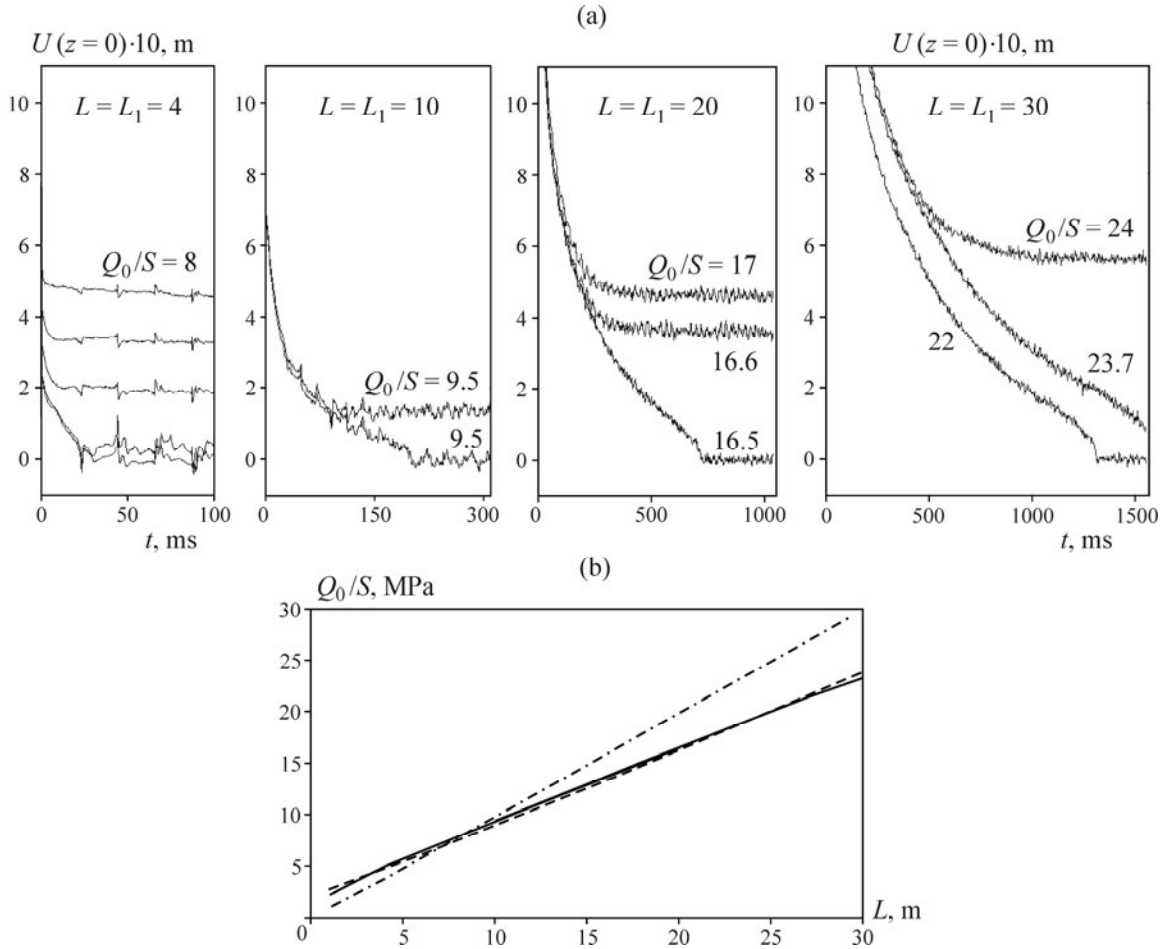

Fig. 10. (a) Oscillograms of the pipe displacement under different impact pulse amplitudes; (b) relationship of the slip-initiated impact pulse amplitude and the pipe length.

In [21], using model with neglected deformability of soil around a pipe, it was shown that, given the indicated parameters, the impact pulse to reach the pipe ends requires fulfillment of the equality $Q_0 / S \approx L$ (dash-dotted curve in Fig. 10b). The calculations with the motion of the external medium taken into account show that when $L > 6$ m, the impact pulse amplitude may be smaller than the above estimate.

CONCLUSIONS

The author has derived analytical solutions of one-dimensional radial problem on pipe displacement in an elastic host medium under axial impact loading. It is shown that the numerical and analytical solutions of the one-dimensional problem accurately coincide. The analytical solutions qualitatively correctly describe the solution of the two-dimensional problem on the elastic interaction of the pipe and host medium.

The finite difference calculations of the plane problem on the elastic interaction of the pipe and soil, with dry friction at the pipe and soil interface, performed within a wide range of input parameters, have shown that:

—for the pipe longer than $L_* / 4$, where $L_* = Q_0 /(\tau_0 P)$, the soil motion is to be taken into account;

—for the pipe shorter than $L_* / 4$, taking into account the motion of soil that interacts with the pipe by the Coulomb law of dry friction weakly influences the results, and the calculation may use simpler models with no regard for the soil motion;

—for the pipe shorter than $2L_*$, slip of the pipe in soil is initiated, i.e. the pipe oscillates elastically in soil;

—the impact pulse amplitude that initiates the slip of the pipe linearly relates with the pipe length;
—the slip value is in inverse proportion to the friction force $F_f = PL\tau_0$.

ACKNOWLEDGMENTS

The author is thankful to Dr. Phys.-Math. Sher E.N. for his interest in the described analytical research.

REFERENCES

1. Kragel'sky, I.V. and Shchedrov, V.S., *Razvitie nauki o trenii. Sukhoe trenie* (Development of the Friction Science. Dry Friction), Moscow: AN SSSR, 1956.
2. Mikhin, N.M., *Vneshnee trenie tverdykh tel* (External Friction of Solids), Moscow: Nauka, 1977.
3. Markeev, A.P., *Dinamika tela, soprikasayushchegosya s tverdoi poverkhnost'yu* (Dynamics of a Body in Touch with a Hard Surface), Moscow: Nauka, 1992.
4. Rozenblat, M.G., *Sukhoe trenie i odnostoronnie svyazi v mekhanike tverdogo tela* (Dry Friction and Unilateral Connections in Solid Mechanics), Moscow: URSS, 2010.
5. Andronov, V.V. and Zhuravlev, V.F., *Sukhoe trenie v zadachakh mekhaniki* (Dry Friction in Mechanical Problems), Moscow–Izhevsk: Inst. Komp. Issled., 2010.
6. Ivanov, A.P., *Osnovy teorii sistem s sukhim treniem* (Foundations of the Theory on Systems with Dry Friction), Moscow–Izhevsk: Inst. Komp. Issled., 2011.
7. Veklich, M.A. and Malyshev, B.M., Propagation of Waves in Elastic Rods in a Medium with Dry Friction, *Zadachi mekhaniki tverdogo deformiruemogo tela* (Problems of the Deformable Solid Mechanics), Moscow: MGU, 1985.
8. Ormonbekov, T.O, *Mekhanika vzaimodeistviya deformiruemykh tel* (Mechanics of Interaction of Deformable Bodies), Frunze: Ilim, 1989.
9. Nikitin, L.V., *Statika i dinamika tverdykh tel s vneshnim sukhim treniem* (Statics and Dynamics of Solids with External Dry Friction), Moscow: Mosk. Litsei, 1998.
10. Yunin, E.K., *Zagadki i paradoksy sukhogo trenia* (Dry Friction: Puzzles and Paradoxes), Moscow: LIBROKOM, 2008.
11. Gersevanov, N.M., *Svainye osnovaniya i raschet fundamentov sooruzhenii* (Pile Foundations and Calculation of Construction Bases), Moscow: Stroivoenmorizdat, 1948.
12. Nikitin, L.V., Dynamics of Elastic Rods with Dry Friction, *Usp. Mekh.*, 1988, vol. 11, no. 4.
13. Nikitin, L.V. and Tyurekhodzhaev, A.N., Behavior of Loaded Elastic Rod in Soil, *Problemy mekhaniki gornykh porod* (Problems of Rock Mechanics), Alma-Ata: Nauka, 1966.
14. Nikitin, L.V., Solid Impact on Elastic Rod with External Dry Friction, *Mekh. Tverd. Tela*, 1967, no. 2.
15. Nikitin, L.V. and Tyurekhodzhaev, A.N., Pipeline Behavior under Impact Wave Action in Soil, *Proc. Int. Conf. Friction, Wear and Lubricants*, Tashkent, 1985.
16. Nikitin, L.V. and Tyurekhodzhaev, A.N., Dry Friction Dampening of Dynamic Loads in a Fiber Composite, *Mekh. Kompozit. Mater.*, 1986, no. 1.
17. Zharkova, N.V. and Nikitin, L.V., Applied Problems of Elastic Rod Dynamics, *Mekh. Tverd. Tela*, 2006, no. 6.
18. Mogilevsky, R.I., Ormonbekov, T.O., and Nikitin, L.V., Dynamics of Rods with Interfacial Dry Friction, *Journal of the Mechanical Behavior of Materials*, 1993, vol. 5, issue 1.
19. Smirnov, A.L., Dynamics of Composite Structures in a Medium under Nonstationary Impact, *Cand. (Phys.-Math.) Dissertation*, Novosibirsk, 1990.
20. Sultanov, K.S., Numerical Solution of Problem of Wave Propagation in Viscoelastic Rod with External Dry Friction, *Mekh. Tverd. Tela*, 1991, no. 6.
21. Aleksandrova, N.I., Numerical-Analytical Investigation into Impact Pipe Driving in Soil with Dry Friction. Part I: Nondeformable External Medium, *Journal of Mining Science*, 2012, vol. 48, no. 5, pp. 856–869.

22. Smith, E.A.L., Pile Driving Analysis by the Wave Equation, *ASCE*, 1960, vol. 86, no. SM4.
23. Cornelius, C.S. and Kubitza, W.K., Experimental Investigation of Longitudinal Wave Propagation in an Elastic Rod with Coulomb Friction, *Exp. Mech*., 1970, vol. 10, no. 4.
24. Wilms, E.V. and Wempner, G.A., Motion of an Elastic Rod with External Coulomb Friction, *Trans. ASME*, 1968, Ser. B, vol. 90.
25. Wilms, E.V., Damping of a Rectangular Stress Pulse in a Thin Elastic Rod by External Coulomb Friction, *J. Acoust. Soc. Am*., 1969, vol. 45, issue 4.
26. Rausche, F., Moses, F., and Goble, G., Soil Resistance Predictions from Pile Dynamics, *ASCE*, 1972, vol. 98, no. SM9.
27. Rausche, F., Likins, G., and Goble, G., A Rational and Usable Wave Equation Soil Model Based on Field Test Correlation, *Proc. Int. Conf. Design and Construction of Deep Foundations*, Orlando, Dec. 1994.
28. Sen, R., Davies, T.G., and Banerjee, P.K., Dynamic Analysis of Piles and Pile Groups Embedded in Homogeneous Soils, *Earthquake Engineering & Structural Dynamics*, 1985, vol. 13, no. 1.
29. Mabsout, M. and Tassoulas, J., A Finite Element Model for the Simulation of Pile Driving, *Int. J. Numer. Methods in Engineering*, 1994, vol. 37, no. 2.
30. Mabsout, M., Reese, L., and Tassoulas, J., Study of Pile Driving by Finite-Element Method, *J. Geotech. Energ*., 1995, vol. 121, no. 7.
31. Paik, K.H., Salgado, R., Lee, J.H., and Kim, B.J., The Behavior of Open- and Closed-Ended Piles Driven into Sands, *ASCE*, 2003, vol. 129, no. 4.
32. Widjaja, B., Wave Equation Analysis and Pile Driving Analyzer for Driven Piles: 18th Floor Office Building Jakarta Case, *Int. Civil Engineering Conf. Towards Sustainable Civil Engineering Practice*, Sarabaya, 2006.
33. Sheng, D., Wriggers, P., and Sloan, S.W., Improved Numerical Algorithms for Frictional Contact in Pile Penetration Analysis, *Computers and Geotechnics*, 2006, vol. 33.
34. Sheng, D., Wriggers, P., and Sloan, S.W., Application of Frictional Contact in Geotechnical Engineering, *International Journal of Geomechanics*, 2007, vol. 7, no. 3.
35. Khelifi, Z., Berga, A., and Terfaya, N., Modeling the Behavior of Axially and Laterally Loaded Pile with a Contact Model, *EJGE*, 2011, vol. 16, bund. N.
36. Petreev, A.M. and Smolentsev, A.S., Blow Energy Transmission from a Striking Machine Element to a Pipe via Adaptor, *Journal of Mining Science*, 2011, vol. 47, no. 6, pp. 787–797.
37. Isakov, A.L. and Shmelev, V.V., Shock-Pulse Transmission on Driving Metal Tubes into the Ground, *Journal of Mining Science*, 1998, vol. 34, no. 1, pp. 73–79.
38. Isakov, A.L. and Shmelev, V.V., Wave Processes when Driving Metal Pipes into the Ground Using Shock-Pulse Generators, *Journal of Mining Science*, 1998, vol. 34, no. 2, pp. 139–147.
39. Beloborodov, V.N., Isakov, A.L., Plavskikh, V.D., and Shmelev, V.V., Modeling Impulse Generation during the Driving of Metals Pipes into Soil, *Journal of Mining Science*, 1997, vol. 33, no. 6, pp. 549–553.
40. Beloborodov, V.N. and Glotova, T.G., Evaluating the Elastic Properties of the Ground, *Journal of Mining Science*, 1998, vol. 34, no. 6, pp. 565–568.
41. Sridhar, N., Yang, Q.D., and Cox, B.N., Slip, Stick, and Reverse Slip Characteristics during Dynamic Fiber Pullout, *Journal of the Mechanics and Physics of Solids*, 2003, vol. 51.
42. Ormonbekov, T.O, *Vzaimodeistvie konstruktsii so sredoi* (Construction and Host Medium Interaction), Frunze: Ilim, 1963.
43. Abdukadyrov, S.A., Stepanenko, M.V., and Pinchukova, N.I., A Method for Numerical Solution of the Dynamics Equations of Elastic Media and Structures, *Journal of Mining Science*, 1984, vol. 20, no. 6, pp. 449–455.
44. Dech, G., *Rukovodstvo po prakticheskomy primenenyu preobrazovaniya Laplasa i Z preobrazovaniya* (Manual on Application of the Laplace and Z Transforms), Moscow: Nauka, 1971.